NETWORKS AND HETEROGENEOUS MEDIA
©American Institute of Mathematical Sciences
Volume **4**, Number **2**, June **2009**
doi:10.3934/nhm.2009.4.303
pp. **303–324**

ADAPTIVE AND NON-ADAPTIVE MODEL PREDICTIVE CONTROL OF AN IRRIGATION CHANNEL

João M. Lemos

INESC-ID/IST/UTL
R. Alves Redol 9, 1000-029 Lisboa, Portugal

Fernando Machado and Nuno Nogueira

INESC-ID
R. Alves Redol 9, 1000-029 Lisboa, Portugal

Luís Rato

Departamento de Informática, Universidade de Évora
Rua Romão Ramalho 59, 7000-671 Évora, Portugal

Manuel Rijo

Núcleo de Hidráulica e Controlo de Canais, Universidade de Évora, Pólo da Mitra
Apartado 94, 7002-554 Évora, Portugal

Abstract. The performance achieved with both adaptive and non-adaptive Model Predictive Control (MPC) when applied to a pilot irrigation channel is evaluated. Several control structures are considered, corresponding to various degrees of centralization of sensor information, ranging from local upstream control of the different channel pools to multivariable control using only proximal pools, and centralized multivariable control relying on a global channel model. In addition to the non-adaptive version, an adaptive MPC algorithm based on redundantly estimated multiple models is considered and tested with and without feedforward of adjacent pool levels, both for upstream and downstream control. In order to establish a baseline, the results of upstream and local PID controllers are included for comparison. A systematic simulation study of the performances of these controllers, both for disturbance rejection and reference tracking is shown.

1. **Introduction.** Irrigation channels are large, spatially distributed structures in which wave propagation phenomena occur. Due to this, when control design is based on lumped parameter approximation models, the interaction among different sections has to be taken into account. On the other way, multivariable control demands the centralization of the information provided by different sensors that may be long distances apart. This naturally rises the issue of evaluating the performance increase due to the use of multivariable, centralized control, versus partially or totally decentralized schemes requiring simpler algorithms.

Another difficulty is posed by the uncertainty in the dynamic models available. Vegetation growing in the banks, mud accumulation and water losses cause changes in model parameters, making the system time-varying in unpredictable ways. As

2000 *Mathematics Subject Classification.* Primary: 93C83, 93C95; Secondary: 93C40, 93A14.
Key words and phrases. Control, Predictive Control, Adaptive Control, Irrigation Channels.

is well known, adaptation is a classical way of tackling the problem of preventing performance degradation when facing significant levels of uncertainty. But again there is a counterpart: Adaptive control may induce complex dynamics and requires an expert to tune its configuration parameters.

The above issues are considered here in relation to a pilot water irrigation channel. The plant used as a prototype is the experimental channel of *Núcleo de Hidráulica e Controlo de Canais* of University of Évora, Portugal. Although a pilot plant, this channel has dimensions (150 m long) and is provided with equipment (sensors, actuators, SCADA interfaces) that allows the experiments performed on it to face problems similar to the ones found in non-pilot channels. For this reason, it has been used in several experimental works as a test bench [14, 15].

Model Predictive Control (MPC) [16] is a popular tool in industry and it appears to be quite suitable to irrigation channel control as well. Indeed, it embodies in an optimization framework important aspects of the problem, *viz.* constraint handling, reference management and accessible disturbances. Furthermore, it provides a flexible tool for controller structuring, including SISO, MISO and MIMO control. In particular, distributed MPC [5] reveals as a powerful tool for distributed control over complex networks. This motivates a systematic study of the performance achievable by both adaptive and nonadaptive MPC, which is the problem considered in the present paper.

1.1. **State of the art.** In recent years, canal control has been a subject of intensive research [18, 17, 15]. This is motivated both by a strong interest on applications and by the scientific challenges that this problem raises.

The core of open surface water distribution canals are the Saint-Venant equations. These form a hyperbolic system of partial differential equations that embody mass and moment conservation laws [6]. Although providing an accurate tool for modelling, these equations are not always adequate for control design due to its complexity and require approximations [21]. As such, a number of control strategies have been designed, including Optimal Control based on LQR methods [9], LPV and gain-scheduling methods [4], Model Predictive Control, either based on linear or nonlinear models, [1, 2, 10], Lyapunov methods [7], Rieman invariants [11] and robust Internal Model Control [13]. A canal with multiple pools is intrinsically a multivariable system, although many practical control implementations are networks of local SISO controllers. This lead to the investigation of issues like stability properties and suboptimal controllers including feedforward effects [22] and the use of augmented lagrangian and decomposition/coordination methods [8].

As in many other plants, a significant difficulty is to obtain the model upon which control design is based. Even if simplified models are used, it is expensive to perform the experiments in order to get the data needed for identification purposes. Furthermore, the dynamics of a real canal is prone to time variations due, *e. g.* to mundane factors such as mud accumulation or lack of gate lubrication. This is a major motivation for the use of adaptive methods as described below.

1.2. **Paper contributions and organization.** In this paper, the performance achieved with both adaptive and non-adaptive Model Predictive Control (MPC) when applied to a pilot irrigation channel is evaluated. Several control structures are considered, corresponding to various degrees of centralization of sensor information, ranging from local upstream control of the different channel pools to multivariable

FIGURE 1. Overall view of the pilot channel and detail of one gate

control using only proximal pools, and centralized multivariable control relying on a global channel model.

In addition to the non-adaptive version, an adaptive MPC algorithm based on redundantly estimated multiple models is considered and tested with and without feedforward of adjacent pool levels, both for upstream and downstream control. In order to establish a baseline, the results of upstream local PID controllers are included for comparison. A systematic simulation study of the performances of these controllers, both for disturbance rejection and reference tracking is shown. Experimental results on the application of adaptive MPC to the pilot canal are presented.

The paper is organized as follows: After the Introduction (section 1) that motivates the problem, performs a synthetic state of the art review and describes the paper contribution and organization, the channel used as a prototype is described in section 2, together with the models used both for simulation and controller design. The control algorithms considered are described in section 3 and the results concerning their comparison are presented in section 4. Experimental results on adaptive MPC are presented in section 5. Finally, section 6 draws conclusions.

2. **The pilot channel.**

The channel considered as a prototype for testing is described hereafter, together with nonlinear and linear incremental models. The nonlinear model aims at representing canal dynamics as accurately as possible and is needed for simulation purposes. In turn, linear incremental models are required by MPC algorithms.

2.1. **Plant description.**

A photograph of the pilot channel is seen in figure 1 and figure 2 shows a schematic longitudinal view.

The automatic channel is controlled by a main computer server equipped with a SCADA system that allows the remote control and monitoring from the central post. This system provides facilities for the export of logged data to text files, that can be then easily imported from post-processing tools like *Matlab*. It may also be connected to a personal computer where a *C*-program is used for real time control.

The channel has four branches (pools) separated by three orifice gates, with the last having an overshoot gate downstream. It is made of concrete with a trapezoidal

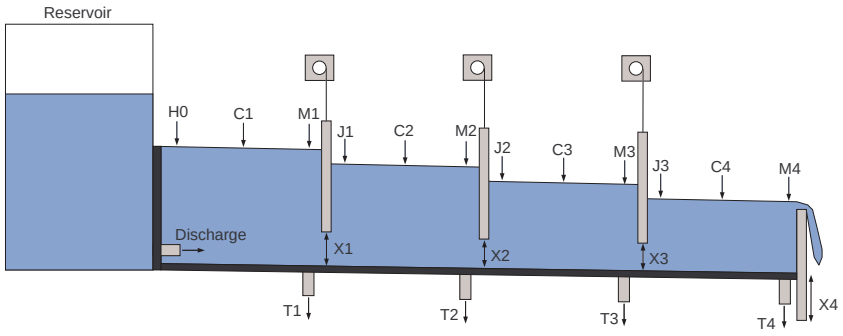

FIGURE 2. Schematics of the automatic channel of NuHCC.

cross section, with 0.15 m of bottom width; side slope 1 : 0.15 (V:H); 0.90 m vertical depth; $1.5 \cdot 10^{-3}$ longitudinal bottom slope. The design flow is $0.09\,\mathrm{m^3 s^{-1}}$.

There are water off-takes downstream from each branch ($T_1, \ldots, T_4$ in figure 2), that are orifices in the channel walls, with additional pipes and valves and equipped with flowmeters. The position of the gates, as marked in figure 2, is denoted by $X_1, \ldots, X_4$.

In order to make possible real time digital control, water level sensors are installed, three for each pool, respectively, at the beginning, middle and end of the pool, as seen in figure 2. Each sensor is installed within an off-line stilling well, a fibrocement pipe with 300 mm of diameter. In this pipe, a curve with 90° and of the same diameter was installed, for the connection to the channel (near the bottom). These sensors allow to record variations around $0.7\,mm$ in the water levels. For gate number i, $i = 1, \ldots, 4$, the upstream level is denoted M_i and the downstream level J_i (figure 2)

The channel inlet is equipped with a motorized flow control valve that delivers a chosen discharge to the input of the channel.

2.2. **Physical model.** In this section the equations that model the dynamics of the channel and the gates are described. A similar model for the same channel is described in [14]. The nonlinear model is used to simulated the plant and to obtain the linearized models required by non-adaptive MPC.

2.2.1. *Saint-Venant Equations.* The open channel flow along each pool is described by the Saint-Venant equations [6], a hyperbolic system of nonlinear partial differential equations. These equations are deduced under the following assumptions:

- the flow is unidimensional;
- the bed slope S_0 of the channel is small enough so one can approximate $\sin(S_0) = S_0$;
- the water density ρ is constant;
- the pressure distribution is hydrostatic;
- the effects of internal viscosity are negligible face to the external friction.

Under these conditions, the equations are:

$$\frac{\partial A}{\partial t} + \frac{\partial Q}{\partial x} = q_l \tag{1}$$

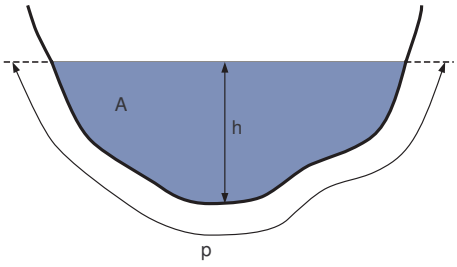

FIGURE 3. channel cross-section showing the hydraulic perimeter

$$\frac{\partial Q}{\partial t} + \frac{\partial Q^2/A}{\partial x} + gA\frac{\partial h}{\partial x} + gA(S_f - S_0) = kq_lV \tag{2}$$

where:

- t time [s]
- x space [m]
- $A(x,t)$ flow cross sectional area [m^2]
- $Q(x,t)$ discharge [m^3s^{-1}]
- $q_l(x,t)$ lateral discharge per unit length [m^2s^{-1}]
- k constant
  inflow: $q_l > 0 \rightarrow k = 0$;
  outflow: $q_l < 0 \rightarrow k = 1$
- g gravitational acceleration [ms^{-2}]
- $h(x,t)$ water level [m]
- $S_f(x,t)$ friction slope
- $V(x,t)$ water velocity [ms^{-1}]

Equation (1) describes mass conservation and equation (2) describes momentum conservation. The friction is modeled using the Manning-Strickler formula:

$$S_f = \frac{Q|Q|n^2}{A^2R^{4/3}} \tag{3}$$

where:

- $R(x,t)$ hydraulic radius [m]
- n Manning coefficient [$m^{-1/3}s$]

The hydraulic radius R is computed using the hydraulic perimeter $P(x,t)$, defined as shown in figure 3, by

$$R = \frac{A}{P} \tag{4}$$

Together with appropriate boundary conditions, these equations fully model the channel and allow to compute the system behavior from a specific initial state (initial flow and water level, $Q(x,0)$ and $h(x,0)$ respectively). The boundary conditions used are restrictions to the discharge at the beginning and the end of the channel ($Q(0,t)$ and $Q(x,t)$, where x is the channel length). The discharge at these points is given by the gate equations. Because of their complexity, there is no analytical solution to these equations for the non-stationary case, and a numerical method ought to be used.

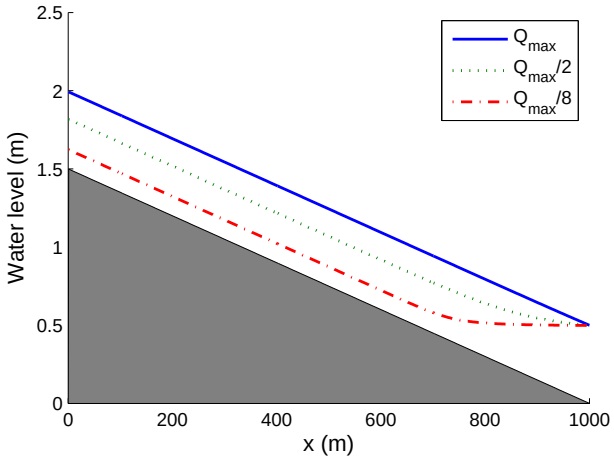

FIGURE 4. Example of backwater curves.

2.2.2. *Stationary Regime.* If both A and Q are assumed to be constant in time, their time derivatives vanish and it is possible to simplify the Saint-Venant equations for this stationary case. After some algebraic manipulation the following equations hold:

$$\frac{\partial Q}{\partial x} = 0 \tag{5}$$

$$\frac{\partial h(x)}{\partial x} = \frac{S_0 - S_f(x)}{1 - F_r^2(x)} \tag{6}$$

in which F_r is the Froude number, computed by:

$$F_r^2 = \frac{Q^2}{g \cdot A^3} \frac{\partial A}{\partial h} \tag{7}$$

It is assumed that the flow is subcritical, *i.e.*, $F_r < 1$. By solving these equations the stationary regime is obtained, which corresponds to a constant flow along the channel and a water level that is derived from eq.(6). The solutions to these equations are called *backwater curves*. Note that in the general case the water level is not constant over the length of the channel, as could be expected. One particular solution of the equations is the one with constant water level, where:

$$S_f(x) = S_0 \tag{8}$$

Figure 4 shows backwater curves obtained with the parameters of the Évora channel, except for length, which is considered to be 1000m, for demonstration purposes. In this case, the downstream water level is considered to be 0.5m and the nominal flow $Q_{max} = 0.09\text{m}^3\text{s}^{-1}$.

These solutions are used in the simulator as initial conditions for the water levels.

2.2.3. *Gate Equations.* In a generic gate, the flow Q passing through the gate depends on the gate position h_{gate}, and the water levels upstream, h_{left}, and downstream, h_{right}, from it:

$$Q = f(h_{left}, h_{right}, h_{gate}) \tag{9}$$

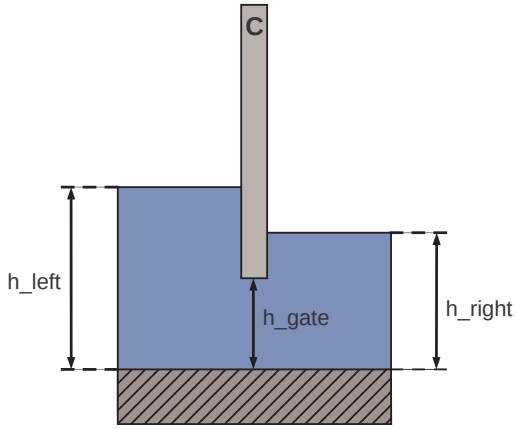

FIGURE 5. Schematic side view of an orifice gate

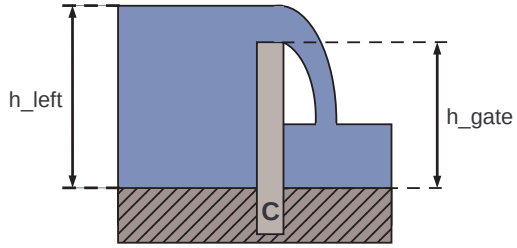

FIGURE 6. Schematic side view of an overshoot gate

In an orifice gate (figure 5), the water flows below the gate, and its characteristic is given by:

$$Q = C_{ds}\, A\, \sqrt{2g\,(h_{left} - h_{right})} \tag{10}$$

where $A(h_{gate})$ [m^2] is the effective area of the orifice and C_{ds} is the gate's discharge coefficient.

In an overshoot gate (figure 6) the water flows over the gate, and the following model [14] is used:

$$Q = B\, C_d\, \sqrt{2g}\,(h_{left} - h_{gate})^{3/2} \tag{11}$$

where B is the gate width.

In both cases, the gates are characterized by the discharge coefficient C_d, that can be determined experimentally.

2.2.4. *Numerical Solution of the Equations.* In order to solve the Saint-Venant equations, one needs to use numerical methods for solving PDEs, because these equations do not have an analytical solution for the non-stationary case. To solve these equations the well known Preissmann scheme [21] is used, which is an implicit method

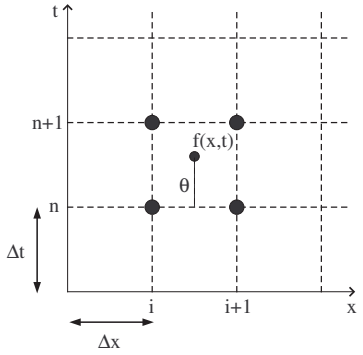

FIGURE 7. Preissmann four-point scheme.

that consists in approximating the space and time derivatives by finite difference in four points (figure 7).

For this sake, a function of t and x, and its derivatives is approximated as follows:

$$f(x,t) \simeq M\, f_j^n = \frac{\theta}{2}\,(f_{i+1}^{n+1} + f_i^{n+1}) + \frac{1-\theta}{2}\,(f_{i+1}^n + f_i^n) \tag{12}$$

$$\frac{\partial f}{\partial x} \simeq D_x\, f_j^n = \theta\,\frac{f_{i+1}^{n+1} - f_i^{n+1}}{\Delta x} + (1-\theta)\,\frac{f_{i+1}^n - f_i^n}{\Delta x} \tag{13}$$

$$\frac{\partial f}{\partial t} \simeq D_t\, f_j^n = \frac{f_{i+1}^{n+1} - f_{i+1}^n + f_i^{n+1} - f_i^n}{2\,\Delta t} \tag{14}$$

Here, i is the spatial index, n is the time index and θ is a weighting constant that has a value between 0 and 1. The choice $\theta = 0.65$ was made. The symbols M, D_x and D_t denote finite difference operators. Replacing the unknown functions in the Saint-Venant equations by the given approximations yields a system of implicit equations that can be solved numerically using the Newton method.

2.2.5. *Modular SIMULINK implementation.* The implementation of the models of the channel and gates was made in *MATLAB/SIMULINK*, using S-functions. An effort was made to allow the resulting model to be modular and easy to adapt to different channels.

A channel pool (branch) is represented by a *SIMULINK* block that has as inputs the boundary conditions for the channel (input and output discharges) and as outputs the water levels upstream, downstream and in the middle of the branch.

A gate is represented by a *SIMULINK* block that has as inputs the water levels upstream and downstream of the gate and the gate opening, and as output the discharge flow through the gate. Two *SIMULINK* blocks were developed, one representing an overshoot gate and another representing an orifice gate.

Figure 7 shows the *SIMULINK* blocks of an orifice gate, of a branch of channel and of an overshoot gate, with the respective input and output signals.

In order to simulate the behavior of a full channel with several pools and gates, multiple *SIMULINK* blocks are connected. Each pool, as well as each gate, is represented by a *SIMULINK* block. In this way, a modular structure is built that allows to easily represent virtually any channel. The output of a "branch" block

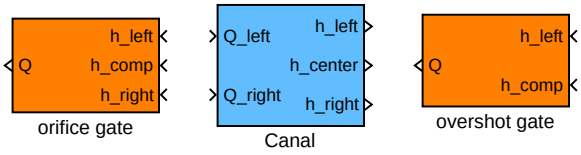

FIGURE 8. The *SIMULINK* blocks developed for building channel models.

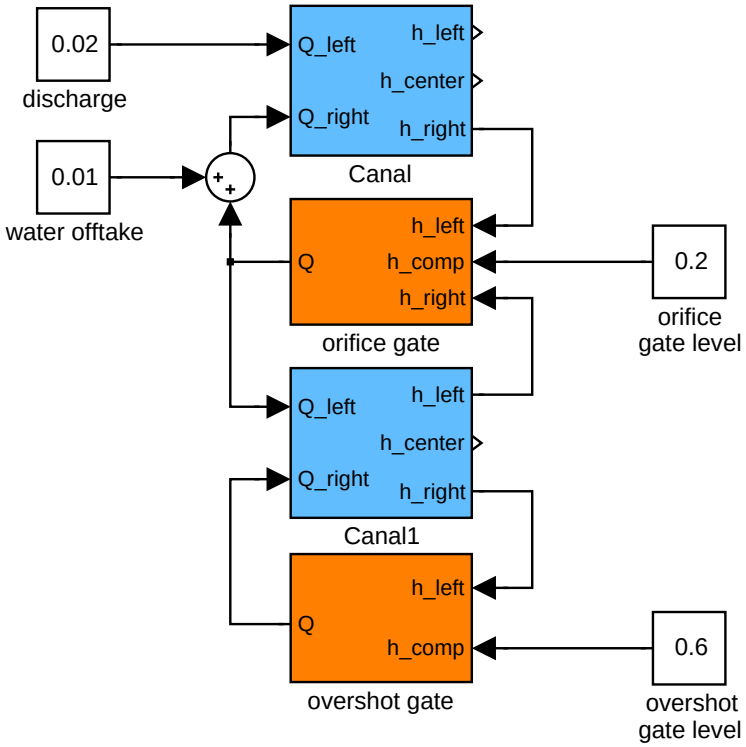

FIGURE 9. Connection between *SIMULINK* blocks to make a 2 pool channel model.

(representing a pool) is connected to the input of the a "gate" block, whose outputs are also connected to the inputs of the same "channel" and to the next "channel" block. The input of a "channel" block can alternatively be connected to any other signal source. Water offtakes downstream of a branch of a channel can be modelled by simply adding the outflow to the pool flow output.

Figure 9 shows an example of the connections between blocks. This model represents two pools connected through an orifice gate. The first pool has a constant discharge input upstream, while the second one has an overshoot gate downstream. There is a water offtake downstream of the first pool. The model of the pilot channel considered is more complicated (having four pools and four gates), but is build according to the same procedure.

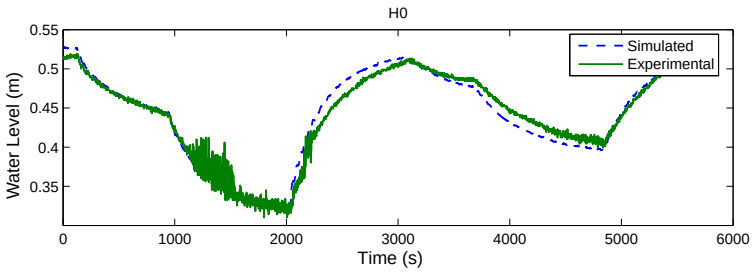

FIGURE 10. Comparison between the experimental and simulated levels for H0.

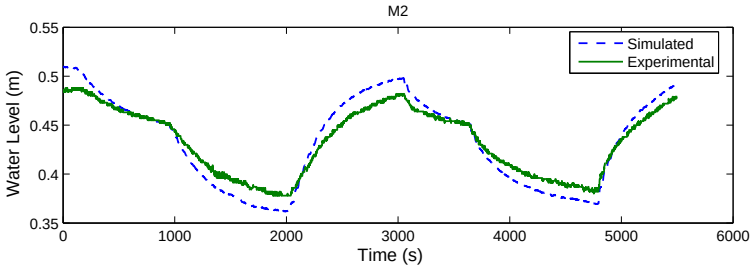

FIGURE 11. Comparison between the experimental and simulated levels for M2.

2.2.6. *Parameter estimation and model validation.* In the mathematical description of the channel a number of parameters need to be estimated from experimental data. Regarding the channel pools only the Manning coefficient is to be estimated since its geometry data can be retrieved from tables. It is also necessary to determine the discharge constants of the gates. These parameters have major impact on the behavior of the complete model, so most attention was set in their calibration.

In order to determine the parameters that most accurately characterize the channel considered, a minimization of the mean square error between the experimental and simulated data was made. It was noticed that experimental data is affected by an offset due to the wrong calibration of the water level sensors. For this reason, sensor offsets have been estimated as well. Another reason for the differences between experimental data and model output is that the *SIMULINK* model does not completely represent the channel in the segment upstream of the gates, that has a geometry different from the one modeled.

Figures 10, 11 and 12 show a comparison between simulated and experimental data. The experiment consisted in the opening and closing of some of the water offtakes, maintaining the gate levels constant. The first water offtake (T1) was opened to $0.005\,\mathrm{m^3 s^{-1}}$, then to $0.01\,\mathrm{m^3 s^{-1}}$, and finally was closed. The same procedure was repeated with the second water offtake (T2). The water levels represented in the figures correspond to levels H0, M2 and J3 in figure 2.

2.3. **Linear incremental model.** A multivariable linear incremental model is needed for the MPC algorithm. In this case, the model inputs are increments

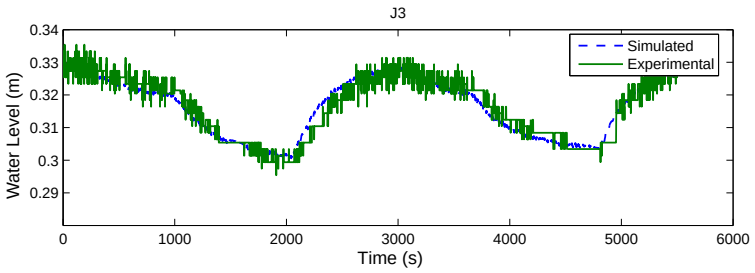

FIGURE 12. Comparison between the experimental and simulated levels for J3.

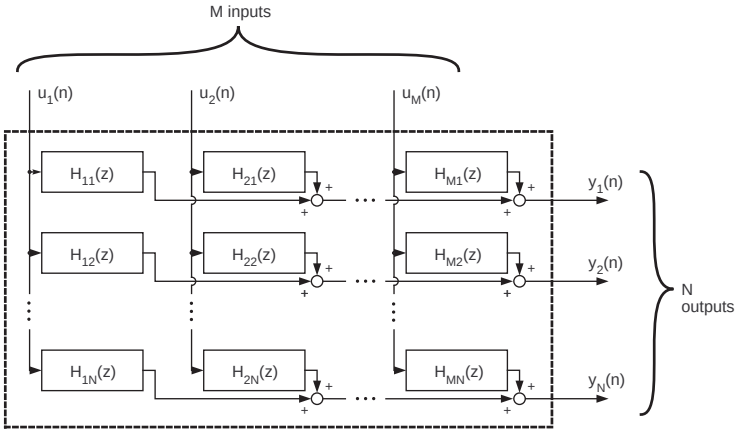

FIGURE 13. Block diagram of the global incremental model.

around the operating point of plant manipulated variables (gate positions, side-take valve positions, and MONOVAR valve position) and the model outputs are the measured incremental variables (3 levels per pool, as shown in figure 2).

In order to obtain the linear incremental model, discrete time transfer functions $H_{i,j}(z)$ relating input number i with output number j were estimated from data generated using the nonlinear model. The sampling time is selected as $5\,s$. This replicates well the canal dynamics and, furthermore, is appropriate for the controllers considered in this paper. From these transfer functions a matrix model was build, with the structure shown in figure 13. Although the resulting model is not of minimal order, this proved to be an adequate approach. The validation of the entries of the incremental model is seen in figure 14. Here, both plots are simulations, one obtained with the nonlinear model and the other with the linear model. The objective is to show that both curves are close, and therefore that the linear model is a good approximation to the nonlinear model, around the operating point considered.

3. **Control.** The channel, whose schematic view is shown on figure 2, is a multivariable system, with 4 manipulated inputs $u_i = X_i$, $i = 1, \ldots, 4$ and 4 outputs

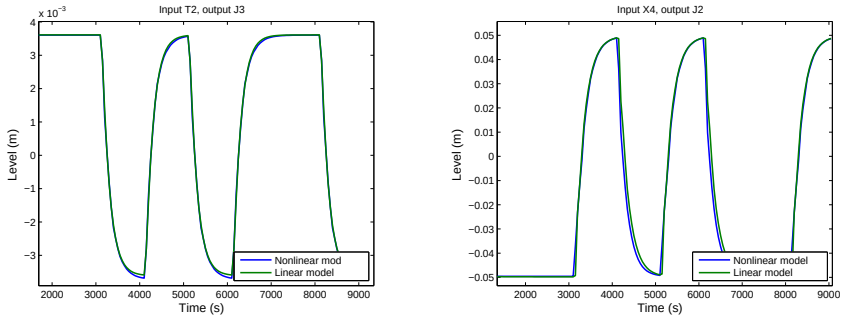

(a) (b)

FIGURE 14. Comparison of the linear incremental and nonlinear models.

given by the upstream levels $y_i = M_i$, $i = 1, \ldots, 4$. Furthermore, the outtakes T_i, $i = 1, \ldots, 4$, are disturbances that may be considered accessible for measure. The control objective consists on acting on the manipulated inputs such that the output level signals have the desired values with a minimum of control effort.

Although this control objective can be attained with a multivariable controller, other structures based on networks of local controllers may be used, with the advantage of requiring simpler communication networks. Hence, hereafter the following control structures are considered:

- *Upstream control.* A SISO controller is associated with each pool and uses as feedback signal the closest upstream level measure *i. e.*, for gate i, controller C_i computes the gate position, X_i, using as feedback signal M_i.
- *Downstream control.* A SISO controller is associated with each pool and uses as feedback signal the closest downstream level measure *i. e.*, for gate i, controller C_i computes the gate position, X_i, using as feedback signal J_i. This type of control applies only to gates 1 to 3.
- *Feedforward from accessible disturbances.* To both the above structures one may add to each manipulated variable a term proportional to the error in other local control loops. This exerts a feedforward action that helps to coordinate the different local controllers. Two possibilities tried hereafter consist on using either the tracking error from the previous pool or the sum of the tracking errors in all the up-stream pools. Using the sum of the tracking errors from up-stream pools is motivated by the fact that it anticipates disturbances that will appear in the future due to correction actions made by the controllers in those pools.
- *Multivariable control based on a proximal model.* This refers to a controller based on a model that only takes into consideration the adjacent pools to the one being considered, using a MISO model.

In this paper, the local controllers are variants of Model Predictive Controllers (MPC). PIDs are also considered in order to establish a base line for comparison.

3.1. **Model predictive control.** Model Predictive Control (MPC) [16] is a well established procedure for process control. Its advantages include the ability to tackle constraints and multivariable problems, yielding robust controllers. Although MPC based on nonlinear models is available [20], linear model based MPC is considered in this work. As is well known, in a deterministic framework, the manipulated variable

is obtained by minimizing the multistep quadratic cost

$$J(k) = \sum_{i=0}^{T_p} [\|(y(k+i) - r(k+i))\|^2_{W_y} +$$

$$+ \sum_{i=0}^{T_u} [\|u(k+i)\|^2_{W_u} + \|\Delta u(k+i)\|^2_{W_{\Delta u}}] \tag{15}$$

subject to operational and state constraints [16]. Here u, y and r are, *viz.*, the vectors of manipulated variables, plant output and reference and W_y, W_u and $W_{\Delta u}$ are matrices of weights, with $\|z\|_Q \stackrel{=}{\triangle} z^T Q z$ for any column vector z and a matrix Q. The parameters T_p and T_u are, respectively, the prediction and the control horizons. The connection between the input and the output is established through a model. In the situation considered, the model consists of a matrix of discrete time transfer functions estimated using data obtained from the nonlinear plant model described in section 2 and corresponding to the nominal operating point. According to the receding horizon principle, only the first element $u(k)$ of the optimal sequence is actually applied to the plant, the whole procedure being repeated at discrete time $k+1$.

3.2. **Adaptive MPC.** Adaptive MPC is obtained by coupling to it an identification procedure to estimate on-line the model parameters. Many possibilities may be considered. Here, a stochastic framework is assumed in order to obtain a generalization of the MUSMAR algorithm [19], closely related to LQ stochastic control.

As discussed in [3], for an ARMAX plant model, the minimization of the modified quadratic criterion

$$J_\infty = E\left[\left(\frac{1}{r}\right)^{2k} \left(y_k^2 + \rho u_k^2\right)\right] \tag{16}$$

with $r < 1$ yields closed-loop systems with guaranteed exponential stability. For a control law minimizing this cost, the variables y_k (process output) and u_k (manipulated variable) must decay to zero at least as fast as r^k, when k grows, and hence the closed loop poles are inside the circle $|z| \leq r$. It is assumed that the innovations in the underlying ARMAX plant model are such that their covariance goes to zero as r^k.

In a predictive control framework, and according to a receding horizon strategy, replace (16) by the multi-step quadratic cost approximation

$$J_T = \frac{1}{2T} E\left[\sum_{k=1}^{T} \left(\frac{1}{r}\right)^{2k} \left(y_{t+k}^2 + \rho u_{t+k-1}^2\right) | I^t\right] \tag{17}$$

where $E[\cdot|I^t]$ denotes the mean conditioned on the $\sigma-$algebra generated by the observations up to time t. This is an approximation to the exact guaranteed exponential stability controller that goes tighter when the horizon T increases. The inclusion of an exponential weight that grows along the horizon relates the algorithm to other receding horizon controllers that impose a constraint on the final state, *e. g.* by using a final penalty in order to guarantee stability with a finite horizon for receding horizon schemes [20].

The MUSMAR adaptive MPC algorithm modified to include an exponential weight and feed-forward from accessible disturbances reads as follows:

Modified MUSMAR with exponential cost

At the beginning of each sampling interval t (discrete time), recursively perform the following steps:

1.Sample plant output, $y(t)$ and compute the tracking error $\tilde{y}$, with respect to the desired set-point $y^*(t)$, by:

$$\tilde{y}(t) = y^*(t) - y(t) \tag{18}$$

2.Using Recursive Least Squares (RLS), update the estimates of the parameters θ_j, ψ_j, μ_{j-1} and ϕ_{j-1} in the following set of predictive models:

$$\tilde{y}(t+j) \approx \theta_j u(t) + \psi_j' s(t) \tag{19}$$

$$u(t+j-1) \approx \mu_{j-1} u(t) + \phi_{j-1}' s(t) \tag{20}$$

$$j = 1, \ldots, T$$

where $\approx$ denotes equality in least squares sense and $s(t)$ is a sufficient statistic for computing the control, hereafter referred as the pseudo-state, given by

$$s(t) = [\tilde{y}(t) \ \ldots \ \tilde{y}(t-n+1) \ u(t-1) \ \ldots \ u(t-m)$$
$$w_1(t) \ \ldots \ w_1(t-n_{w1}) \ \ldots \ w_N(t) \ \ldots \ w_N(t-n_{wN}) \ 1]' \tag{21}$$

where the w_i are samples of auxiliary variables such as intermediate process variables or accessible disturbances. Since, at time t, $\tilde{y}(t+j)$ and $u(t+j)$ are not available for $j \geq 1$, for the purpose of estimating the parameters, the variables in (19,20) are delayed in block of T samples. The estimation equations are thus,

$$K(t) = \frac{P(t-1)\varphi(t-T)}{1 + \varphi'(t-T)P(t-1)\varphi(t-T)[1-\beta(t)]} \tag{22}$$

$$P(t) = [I - K(t)\varphi'(t-T)(1-\beta(t))]P(t-1) \tag{23}$$

with, for $j = 1, \ldots, T$:

$$\hat{\Theta}_j(t) = \hat{\Theta}_j(t-1) + K(t)[y(t-T+j) - \hat{\Theta}_j(t-T)'\varphi(t-T)] \tag{24}$$

and, for $j = 1, \ldots, T-1$:

$$\hat{\Omega}_j(t) = \hat{\Omega}_j(t-1) + K(t)[u(t-T+j) - \hat{\Omega}_j(t-T)'\varphi(t-T)] \tag{25}$$

In these equations, $\hat{\Theta}_j$ represents the estimate of the parameter vector of the output predictors, given at each discrete time and for each predictor j by

$$\hat{\Theta}_j = [\theta_j \ \ \psi_j']'$$

and $\varphi(t-T)$ represents the regressor, common to all predictors, given by

$$\varphi(t-T) = [u(t-T) \ s'(t-T)]'$$

Similarly, $\hat{\Omega}_j$ represents the estimate of the parameter vector of the input predictors, given at each discrete time and for each predictor j by

$$\hat{\Omega}_j = [\mu_j \ \ \phi_j']'$$

Note that, since the regressor $\varphi(t-T)$ is common to all the predictive models, the Kalman gain update (22) and the covariance matrix update (23) are also common to all the predictors and need to be performed only once per time iteration. This greatly reduces the computational load.

The variable $\beta(t)$ denotes the quantity of information discarded in each iteration, being given according to a directional forgetting scheme [12] by

$$\beta(t) = 1 - \lambda + \frac{1-\lambda}{\varphi'(t-T)P(t-1)\varphi(t-T)} \tag{26}$$

where the forgetting factor λ is a constant to be chosen between 0 (complete forgetting) and 1 (no forgetting) that determines the rate of forgetting in the direction of incoming information. In practice, a factorized version is used to implement equations (22, 23).

3. Apply to the plant the control given by

$$u(t) = f's(t) + \eta(t) \tag{27}$$

where η is a white dither noise of small amplitude and f is the vector of controller gains, computed from the estimates of the predictive models by

$$f = -\frac{1}{\alpha}\left(\sum_{j=1}^{T}\left(\frac{1}{r}\right)^{2j}\theta_j\psi_j + \rho\sum_{j=1}^{T-1}\left(\frac{1}{r}\right)^{2j}\mu_j\phi_j\right) \tag{28}$$

with the normalization factor α given by

$$\alpha = \sum_{j=1}^{T}\left(\frac{1}{r}\right)^{2j}\theta_j^2 + \rho\left(1 + \sum_{j=1}^{T-1}\left(\frac{1}{r}\right)^{2j}\mu_j^2\right) \tag{29}$$

Here, r is the inverse of the basis of the exponential weight. In other words, r is the radius of the circle to which the closed-loop poles are confined by the algorithm.

4. **Control algorithm comparison.** The control algorithms and structures described on section 3 are compared hereafter when applied to the pilot channel considered. In all the tests performed, the sampling interval T_s was 5 s as mentioned in section 2.3. For all the non-adaptive MPC controllers, $T_p = 15$, $T_u = 10$. As such, the MPC takes decisions on the manipulated variable based on pool level predictions that go as far as $T_p \times T_s = 75\,s$ ahead of current time. This was found to be an appropriate value from the point of view of controller performance.

The weight matrices depend on the type of controller. For the multivariable MPC with global model the following choice was made:

$$Q_y = diag\{0.1,\ 0.1,\ 0.1,\ 0.1\}\quad Q_u = diag\{1,\ 1,\ 1,\ 3\}\quad Q_{\Delta u} = diag\{0.7,\ 0.7,\ 1,\ 4\}$$

For MUSMAR, $T = 10$, $\rho = 0.01$, $n = 3$, $m = 2$, $r = 1$ and $\lambda = 0.995$.

An overall view of the performance yielded by the different control algorithms considered is shown in Table 1. For each control structure, this table shows the results both for reference tracking and for disturbance rejection. For reference tracking the reference level for pools 1 and 3 is made to vary as a square wave whose value changes asynchronously, while the reference for pools 2 and 4 is kept constant. For the sake of illustration, figure 15 shows the results for multivariable MPC with a global model, and figure 17 shows the results for MUSMAR for reference tracking.

For the disturbance rejection test all the pool level set-points are kept constant. Disturbances are induced by making the offtakes of pools 1 and 3 to vary, while the offtakes of pools 2 and 4 are kept closed. Figure 16 shows the results for multivariable MPC with a global model.

Table 1 shows the variance for the tracking error and the manipulated variable in units of $[m^2]$.

The resulting performances are of the same order of magnitude. The best performance for reference tracking is obtained with multivariable MPC with a global model. This is expected since the different pools strongly interact: A change in the set-point of pool 1 induces disturbances in the other pool levels that, in turn, disturb pool 1. Hence, it is not surprising that MPC with the proximal model (a

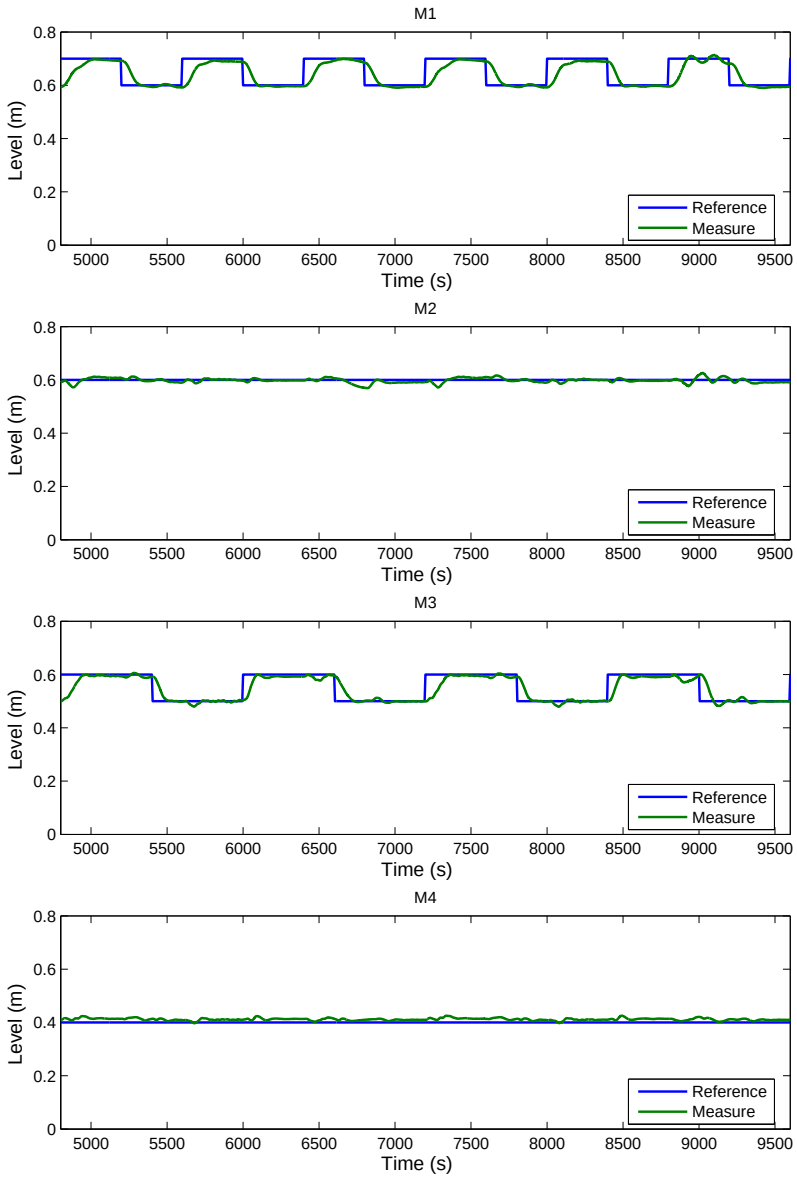

FIGURE 15. Set-point tracking by MPC with global model. Compare with fig. 17.

local controller that takes into account the movement of the gates of the neighborhood pools) leads to a performance between the one of the local MPC controllers (*i. e.* 4 SISO MPC, one for each gate, with to feedforward terms) and the one of multivariable MPC with the global model.

When using a network of local controllers, the inclusion of feedforward clearly improves the performance. Feedforward terms may be computed in several ways. The one that leads to best results was to use as feedforward signal the sum of the tracking errors from the preceding pools (*i. e.* no feedforward for pool 1,

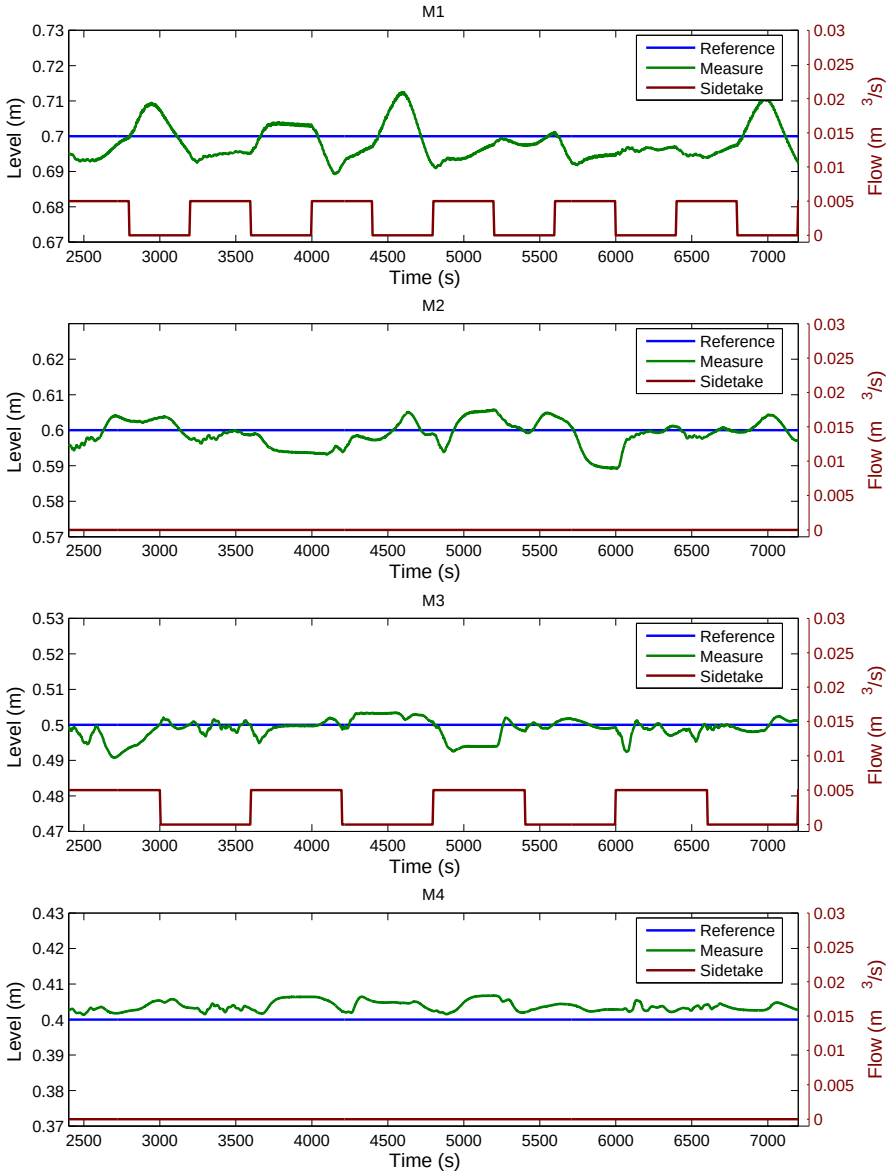

FIGURE 16. Disturbance rejection by MPC with global model. The signal at the bottom of each graphic is the outtake flow of the corresponding pool.

feedforward from the tracking error of pool 1 to pool 2, feedforward from the sum of tracking errors of pools 1 and 2 for pool 3 and so on).

Although not apparent in Table 1, handling rate constraints in the manipulated variables was a major issue since the gate movement presents a slew-rate limitation. This can be done by including a penalty term in the cost functional (15).

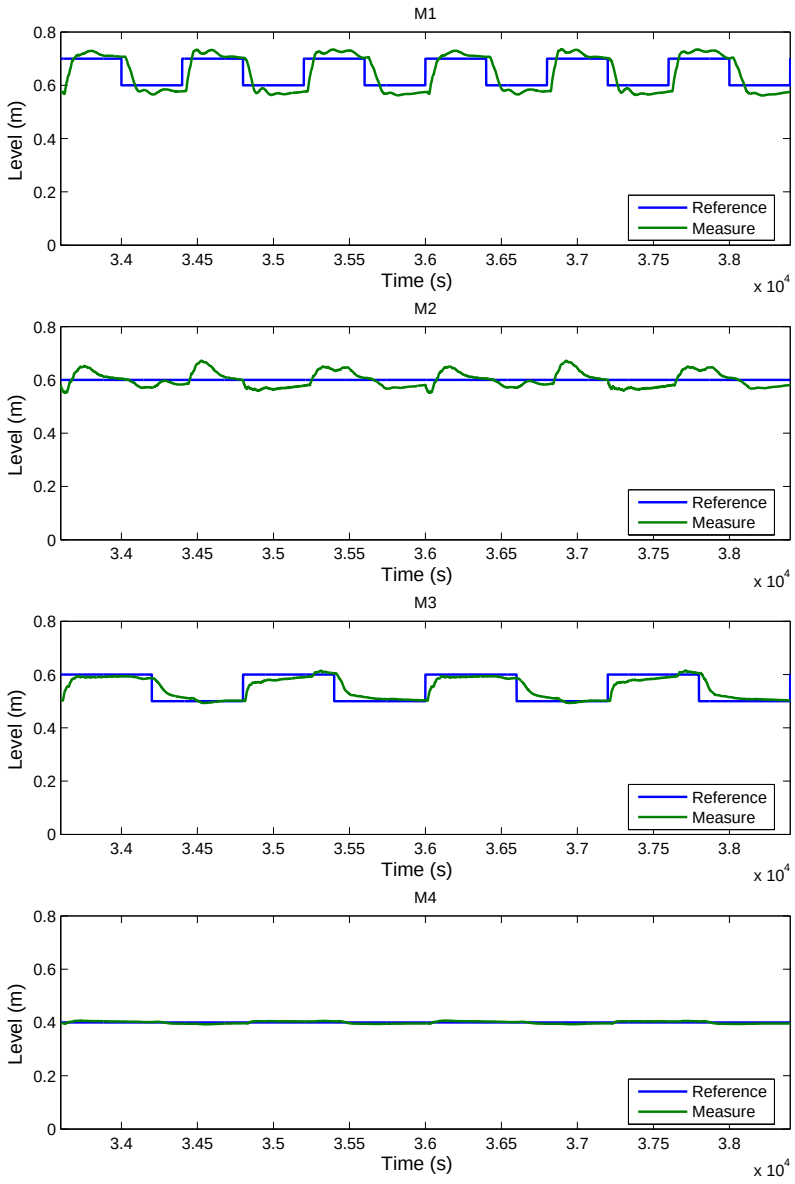

FIGURE 17. Set-point tracking by MUSMAR with long distance upstream control and feedforward from accessible disturbances. Compare with fig. 15.

Another possibility, that only applies to the non-adaptive MPC controllers considered, consists in explicitly imposing a constraint on the maximum rate of change of the manipulated variable.

Although MUSMAR does not present the best performance, its adaptation features make it a quite useful tool in practical situations. Indeed, the good performance of non-adaptive controllers depends on a fixed tuning (made through a plant model valid at an operating point for MPC, that is costly to obtain). If the channel

Controller		Results for ref. tracking		Results for disturb. reject.	
		Average quadr. error	Average quadr. act.	Average quadr. error	Average quadr. act.
PID	upstream	0.0400	1.12×10^{-3}	0.0082	0.47×10^{-3}
	upstream with feed-forward	0.0492	1.34×10^{-3}	0.0063	0.50×10^{-3}
MUSMAR	upstream	0.0717	0.51×10^{-3}	0.0190	0.25×10^{-3}
	upstream with accessible dist.	0.0670	0.67×10^{-3}	0.0156	0.48×10^{-3}
	upstream with added access. dist.	0.0570	0.41×10^{-3}	0.0163	0.20×10^{-3}
	downstream	0.0593	0.66×10^{-3}	0.0103	0.77×10^{-3}
	downstream with accessible dist.	0.0468	0.43×10^{-3}	0.0093	0.47×10^{-3}
MPC	upstream	0.0899	0.76×10^{-3}	0.0205	0.38×10^{-3}
	with proximal model	0.0487	0.47×10^{-3}	0.0117	0.28×10^{-3}
	with global model	0.0250	0.25×10^{-3}	0.0097	0.20×10^{-3}

TABLE 1. Control method comparison. Units are $[m^2]$.

dynamics change, *e. g.* due to mud accumulation, vegetation growth or operating point change) MUSMAR will be able to retune its gains but constant controllers will not.

5. **Experimental results with adaptive MPC.** Figs. 18 and 19 show the simultaneous proximal upstream level control of pools 1 and 2 using the adaptive MPC algorithm. After the extinction of the adaptation transient for pool 1, the controller for pool 2 starts (remark that the time origin for the two graphics is the same). The gates for pools 3 and 4 are kept at constant positions.

After an initial adaptation transient in pool 2 (lasting for about the first 50 samples), the gains converge to what is seen by the algorithm as their optimal values, and the algorithm proceeds then normaly (figure 19). During the transient, the upstream level of pool 2 raised to a temporary incorrect control action and, in turn, this caused pool 1 upstream level to raise. The local controller of pool 1 rejected

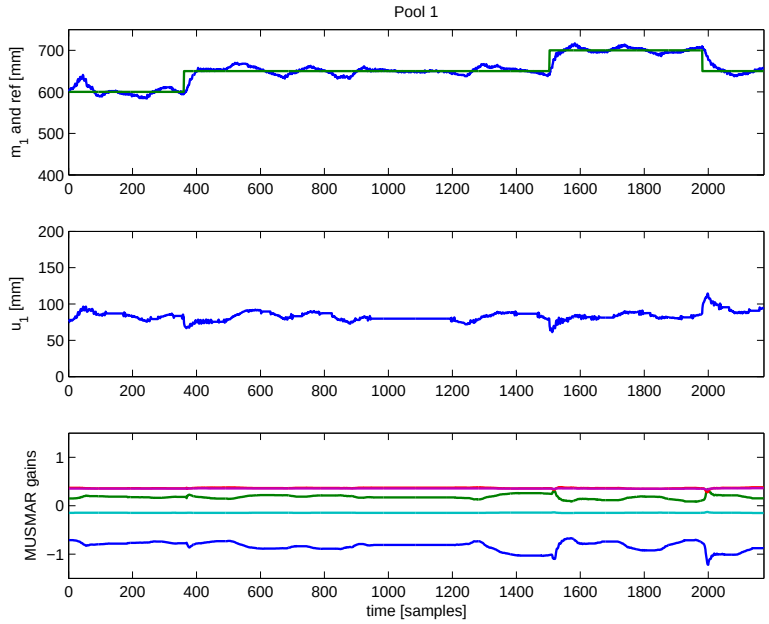

FIGURE 18. Experimental results with adaptive MPC. Simultaneous level control of two pools – pool 1. Level and reference (up), manipulated variable (middle) and controller gains (below).

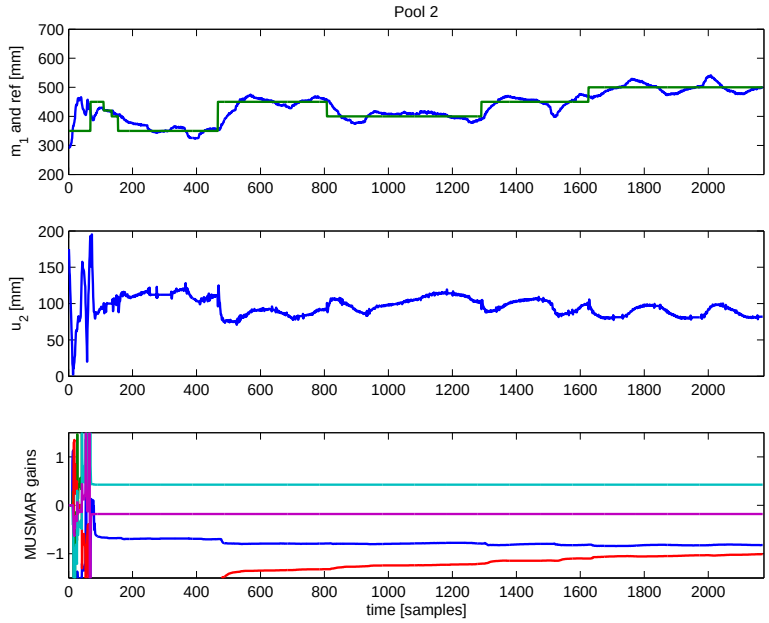

FIGURE 19. Experimental results with adaptive MPC. Simultaneous level control of two pools – pool 2. Level and reference (up), manipulated variable (middle) and controller gains (below).

this disturbance by slightly oppening its gate (figure 18). The corresponding gains were not much disturbed from their convergence values.

6. **Conclusions.** A comparison of different, adaptive and non-adaptive, Model Predictive Control (with linear models) structures has been made when applied to a 4 pool pilot water delivery channel. For that sake, simulations have been made using a non-linear channel model, validated against experimental plant data. The non-linear model served not only the purpose of replacing the plant in the simulations, but it was also used to generate the linear incremental models required by MPC.

The controller with the best performance, either for regulation and set-point tracking, is the multivariable MPC. This not only superseeds controllers based on PID, but has the advantage of providing a systematic design procedure. MPC with a global model requires the concentration of plant signals in one point. If a distributed solution is sought, a possibility is to use MPC based on a MISO model that takes into consideration the positions of adjacent gates. The resulting performance lays between upstream local control, using 4 MPC's with local models and MPC with a global model and may be an interesting choice if a distribution solution is sought.

Channel dynamic characteristics may change with time, suggesting the use of adaptive MPC. Among several other possibilities, the MUSMAR algorithm has been used with a modification to include feedforward from tracking errors, taken as accessible disturbances. Although not presenting the best performance, this option requires less tuning effort, in particular if successive adjustments are to be made. The adaptive MPC was demonstrated experimentally.

REFERENCES

[1] K. Akouz, A. Benhammou, P. O. Malaterre, B. Dahhou and G. Roux, *Predictive control applied to ASCE canal 2*, Proc. IEEE Conf. System, Man and Cybernetics, San Diego, USA, 1998.

[2] E. Arnold and H. Puta, *Nonlinear model predictive control for operational management of a water system*, Proc. European Control Conference, ECC'99, Karlsruhe, Germany, 1999.

[3] K. J. Åstrom and B. Wittenmark, "Computer Controlled Systems," Prentice Hall Inc., 1997.

[4] Y. Bolea, V. Puig, J. Blesa, M. Gomez and J. Rodellar, *LPV vs. multi-model PI(D) gain-scheduling applied to canal control*, Proc. XVI IFAC World Congress, Praha, Czech Republik, 2005.

[5] E. Camponogara, D. Jia, B. Krogh and S. Talukdar, *Distributed model predictive control*, IEEE Control Systems Magazine, **22** (2002), 44–52 .

[6] M. H. Chaudry, "Open-Channel Flow," Prentice Hall Inc., 1993.

[7] J. M. Coron, B. d'Andrea Novel and G. Bastin, *A Lyapunov approach to control irrigation canals modeled by Saint-Venant equations*, Proc. European Control Conference, ECC'99, Karlsruhe, Germany, 1999.

[8] El Fawal, D. Georges and G. Bornard, *Optimal control of complex irrigation systems via decomposition-coordination and the use of augmented Lagrangian*, Proc. 1998 IEEE Int. Conf. Systems, Man and Cybernetics, San Diego, CA, 1998.

[9] A. Garcia, M. Hubbard and J. J. de Vries, *Open channel transient flow control by discrete time LQR methods*, Automatica, **28** (1992), 255–264.

[10] M. Gomez, J. Rodellar and J. A. Mantecon, *Predictive control method for decentralized operation of irrigation canals*, Applied Mathematical Modelling, **26** (2002), 1039–1056.

[11] J. de Halleux, C. Prieur, J.-M. Coron, B. d'Andréa-Novel and G. Bastin, *Boundary feedback control in networks of open channels*, Automatica, J. IFAC, **39** (2003), 1365–1376.

[12] R. Kulhavy, *Restricted exponential forgetting in real time identification*, Automatica, **23** (1987), 589–600.

[13] X. Litrico, *Robust IMC flow control of SIMO dam-river open-channel systems*, IEEE Trans. on Control Systems Technology, **10** (2002), 432–437.

[14] X. Litrico, V. Fromion, J.-P.Baume and M. Rijo, *Modeling and PI control of an irrigation canal*, Proc. European Control Conference, Cambridge, U. K., 2003.

[15] X. Litrico, V. Fromion, J.-P. Baume, C. Arranja and M. Rijo, *Experimental validation of a methodology to control irrigation canals based on Saint-Venant equations*, Control Eng. Practice, **13** (2005), 1425–1437.

[16] J. M. Maciejowski, "Predictive Control with Constraints," Prentice Hall, 2002.

[17] P. O. Malaterre and B. P. Baume, *Modeling and regulation of irrigation canals: Existing applications and ongoing researches*, Proc. IEEE Conf. System, Man and Cybernetics, San Diego, USA, 1998.

[18] I. Mareels, E. Weyer, S. K. Ooi, M. Cantoni, Y. Li and G. Nair, *Systems engeneering for irrigation systems: Successes and challenges*, Proc. 16th IFAC World Congress, Praha, Czech Rep., 2005.

[19] E. Mosca, G. Zappa and J. M. Lemos, *Robustness of multipredictor adaptive regulators: MUSMAR*, Automatica, **25** (1989), 521–529.

[20] G. de Nicolao, L. Magni and R. Scattolini, *Theoretical issues in nonlinear predictive control*, in "Nonlinear Model Predictive Control," 3-22, Birkhäuser, 2000.

[21] S. K. Ooi, M. P. M. Kruzen and E. Weyer, *On physical and data driven modelling of irrigation cahannels*, Control Eng. Practice, **13** (2005), 461–471.

[22] I. G. Welz, X. Litrico, V. Fromin, M. Rijo and P. O. Malaterre, *Stability and performance analysis of classical decentralized control of irrigation canals*, Proc. XVI IFAC World Congress, Praha, Czech Republik, 2005.

Received October 2008; revised February 2009.

E-mail address: jlml@inesc.pt
E-mail address: fermac@ramses.inesc.pt
E-mail address: nunog@ramses.inesc.pt
E-mail address: lmr@di.uevora.pt
E-mail address: rijo@uevora.pt